Research Article

Molecular Cancer Therapeutics

Endocytosis of PEGylated Agents Enhances Cancer Imaging and Anticancer Efficacy

Kuo-Hsiang Chuang[1], Hsin-Ell Wang[7], Fang-Ming Chen[3], Shey-Cherng Tzou[2], Chiu-Min Cheng[2], Ya-Chen Chang[2], Wei-Lung Tseng[4,5], Jentaie Shiea[4,5], Shiu-Ru Lin[6], Jaw-Yuan Wang[3], Bing-Mae Chen[8], Steve R. Roffler[8], and Tian-Lu Cheng[2,3,5]

Abstract

PEGylated nanoparticles and macromolecules are increasingly used in cancer imaging and anticancer treatment. The role of receptor-mediated endocytosis in the efficacy of these agents, however, has not been clearly defined. Here, we developed a matched pair of endocytic and nonendocytic receptors to directly and unambiguously assess this issue. The ligand-binding domains of the low-density lipoprotein receptor (LDLR) or a truncated LDLR lacking the NPXY endocytosis motif (ΔLDLR) were replaced with an anti–polyethylene glycol antibody (αPEG) to form endocytic αPEG-LDLR and nonendocytic αPEG-ΔLDLR receptors. The receptors were stably expressed at similar levels on the surface of HCC36 cells. HCC36/αPEG-LDLR cells, but not HCC36/αPEG-ΔLDLR cells, rapidly endocytosed PEG-quantum dots and PEG-liposomal doxorubicin (Lipo-Dox) *in vitro* and *in vivo*. Lipo-Dox was significantly more cytotoxic to HCC36/αPEG-LDLR cells than to HCC36/αPEG-ΔLDLR cells. HCC36/αPEG-LDLR tumors also accumulated significantly more PEGylated near-IR probes (PEG-NIR797) and PEG-liposomal-^{111}In than HCC36/αPEG-ΔLDLR tumors *in vivo*. Furthermore, Lipo-Dox more significantly suppressed the growth of established HCC36/αPEG-LDLR tumors as compared with HCC36/αPEG-ΔLDLR tumors. Our data show that endocytosis of PEGylated probes and drugs enhances both cancer imaging and anticancer efficacy, indicating that endocytic receptors are superior targets for the design of cancer imaging probes and immunoliposomal drugs. *Mol Cancer Ther; 9(6); 1903–12.* ©*2010 AACR.*

Introduction

Extensive efforts are under way to develop nanoparticles, macromolecules, and proteins that can selectively accumulate in the tumor microenvironment for improved detection and treatment of cancer. Polyethylene glycol (PEG), a flexible polymer, is often covalently attached to these agents to reduce unintended uptake by normal tissues, decrease systemic toxicity, prolong circulation time in the blood, and enhance tumor accumulation (1–5). A prominent example of a PEGylated nanoparticle is PEG-liposomal doxorubicin (Lipo-Dox), which has been approved by the Food and Drug Administration for clinical treatment of ovarian and breast carcinomas and Kaposi's sarcoma (6, 7). Tumor-binding ligands such as peptides (8, 9) and antibodies (10, 11) may be conjugated to the distal terminus of PEGylated nanoparticles and macromolecules to increase targeting specificity. Thus far, various tumor-associated antigens or receptors have been validated as targets for PEGylated compounds, especially for immunoliposomes (10–15). These tumor-associated antigens or receptors can be either endocytic or nonendocytic.

Although PEGylated nanoparticles such as immunoliposomes have shown good clinical activity and promising results in experimental cancer models, it is still unclear how much endocytosis contributes to their anticancer activity. For example, some studies indicate that liposomal drugs targeted to noninternalizing markers facilitate release of drug near the cell surface over time, resulting in bystander toxicity to nearby tumor cells (16, 17). However, the diffusion and redistribution of released drug away from the tumor site may be faster than the speed of drug entry into tumor cells, thus decreasing

Authors' Affiliations: [1]Graduate Institute of Medicine and [2]Department of Biomedical Science and Environmental Biology, Kaohsiung Medical University; [3]Cancer Center, Department of Surgery, Kaohsiung Medical University Hospital; [4]Department of Chemistry, National Sun Yat-Sen University; [5]National Sun Yat-sen University-Kaohsiung Medical University Joint Research Center; [6]Bio-medical Developmental Research Center, School of Medical and Health Fooyin University, Kaohsiung, Taiwan; [7]Faculty of Biomedical Imaging and Radiological Sciences, National Yang-Ming University; and [8]Institute of Biomedical Sciences, Academia Sinica, Taipei, Taiwan

Note: Supplementary material for this article is available at Molecular Cancer Therapeutics Online (http://mct.aacrjournals.org/).

K-H. Chuang and H-E. Wang contributed equally to this work.

Corresponding Authors: Tian-Lu Cheng, Department of Biomedical Science and Environmental Biology, Kaohsiung Medical University, 100 Shih-Chuan 1st Road, Kaohsiung, Taiwan. Phone: 886-7-3121101-2697; Fax: 886-7-3227508. E-mail: tlcheng@kmu.edu.tw, or Steve R. Roffler, Institute of Biomedical Sciences, Academia Sinica, Academia Road, Section 2, No. 128, Taipei 11529, Taiwan. Phone: 886-2-2652-3079; Fax: 886-2-2782-9142. E-mail: sroff@ibms.sinica.edu.tw

doi: 10.1158/1535-7163.MCT-09-0899

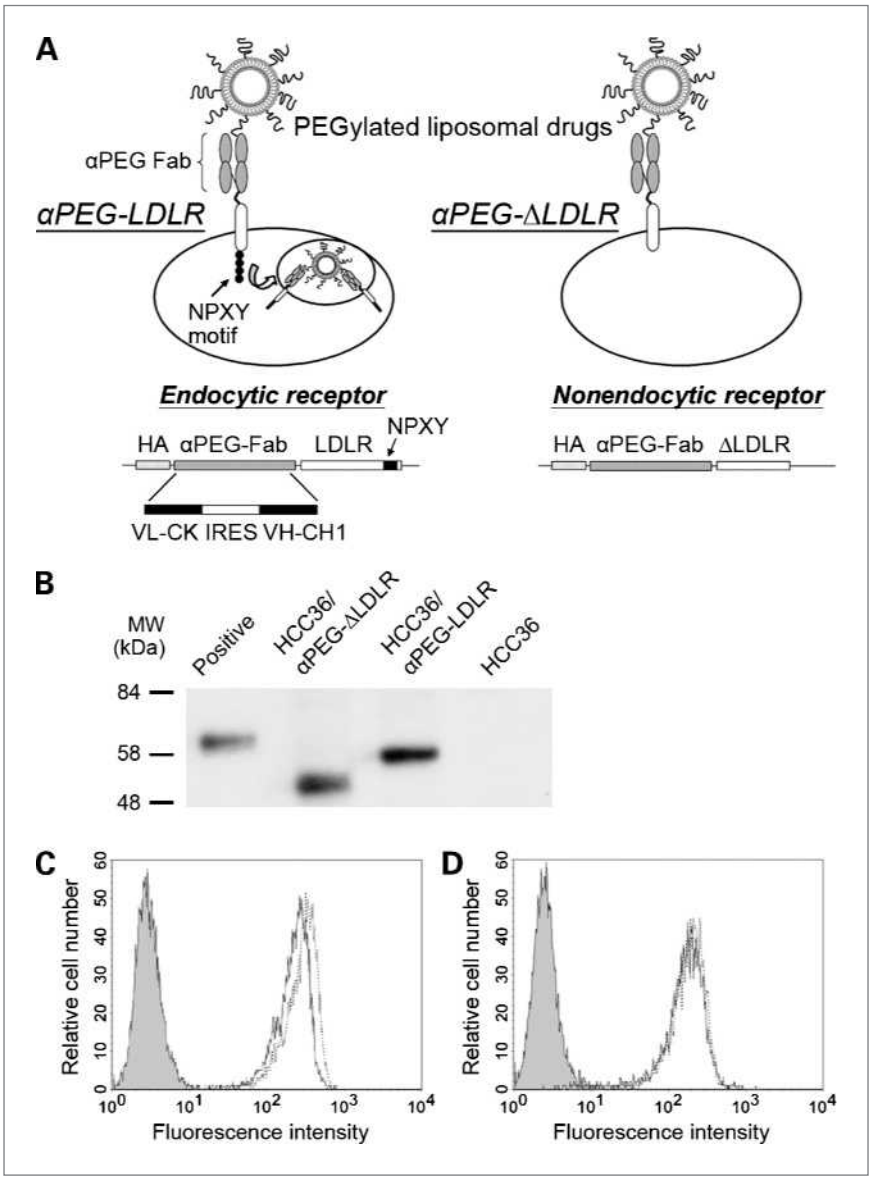

Figure 1. Surface display of functional αPEG receptors. A, schematic representation of endocytic (αPEG-LDLR) and nonendocytic (αPEG-ΔLDLR) receptors. The endocytic receptor gene includes, from NH_2 to COOH termini, an immunoglobulin signal peptide, an HA epitope, the αPEG Fab fragment, and the C-like extracellular, transmembrane, and cytosolic domains of the human LDLR. The organization of the nonendocytic receptor was identical except for the deletion of the NPXY motif from the cytoplasmic tail of the LDLR. B, Western blot analysis of HCC36 cells expressing αPEG-LDLR and αPEG-ΔLDLR receptors using horseradish peroxidase–conjugated goat anti-mouse IgM μ-chain. Lane 1, AGP3 IgM antibody as positive control; lane 2, HCC36/αPEG-ΔLDLR cells; lane 3, HCC36/αPEG-LDLR cells; lane 4, HCC36 cells. C, HCC36/αPEG-LDLR (solid line), HCC36/αPEG-ΔLDLR (dashed line), and HCC36 (filled histogram) cells were analyzed by flow cytometry using a specific antibody to the HA epitope to assess surface expression or stained with PEG-QDs to assess the PEG-binding activity of the receptors (D).

treatment efficiency (18, 19). Other experimental evidence supports the hypothesis that targeting immunoliposomes to endocytic receptors results in better delivery of anticancer agents into cancer cells for enhanced therapeutic efficacy (10–13). Improved treatment efficiency was largely attributed to enhanced cellular internalization of drugs rather than to increased accumulation in tumors (20, 21). Although most experimental results tend to support a role for receptor-mediated endocytosis in the anticancer efficacy of nanoparticles, previous studies have lacked a complementary control (a nonendocytic receptor) and may not provide direct and unbiased evidence to prove this hypothesis. Likewise, it remains unclear whether endocytosis of imaging probes can increase tumor accumulation and detection sensitivity (22–26).

In this report, we sought to (*a*) develop universal cell-surface receptors for PEGylated molecules and (*b*) directly address whether receptor-mediated endocytosis can enhance the accumulation and efficacy of PEGylated imaging and therapeutic agents. We describe a matched pair of endocytic and nonendocytic anti-PEG receptors in which a novel anti-PEG antibody was fused to a truncated low-density lipoprotein receptor (LDLR) and a truncated LDLR (ΔLDLR) lacking the NPXY signal motif for endocytosis (refs. 27, 28; Fig. 1A). Expression of these universal anti-PEG receptors on HCC36 hepatocellular carcinoma cells allowed us to unambiguously begin to define the role of endocytosis in the *in vitro* and *in vivo* efficacy of PEGylated imaging and therapeutic compounds.

Materials and Methods

Materials and reagents

Lipo-Dox was purchased from Taiwan Tung Yang Biopharm Company Ltd. Lipo-Dox contains 2 mg/mL doxorubicin and 14 mol/mL phospholipids. Its lipid composition is DSPC, cholesterol, and PEG-DSPE (molar ratio 3:2:0.3). Lipo-Dox has an average particle size of 104.2 ± 28.3 nm as described previously (29). The synthesis of PEG-liposomal-^{111}In (Lipo-^{111}In) has been described (30). Lipo-^{111}In has the same lipid composition and similar particle size as Lipo-Dox.

Cells and animals

Human HCC36 hepatocellular carcinoma cells (American Type Culture Collection) were cultured in DMEM (Sigma-Aldrich) supplemented with 10% heat-inactivated bovine calf serum, 100 units/mL penicillin, and 100 μg/mL streptomycin at 37°C in an atmosphere of 5% CO_2. Specific pathogen-free female BALB/c nude mice were obtained from the National Laboratory Animal Center, Taipei, Taiwan. All animal experiments were done in accordance with institutional guidelines and approved by the Animal Care and Use Committee of the Kaohsiung Medical University.

Construction and transduction of the endocytic αPEG-LDLR and the nonendocytic αPEG-ΔLDLR receptors

The V_L-Cκ and V_H-C_{H1} domains of an anti-PEG IgM monoclonal antibody (αPEG) were cloned from cDNA prepared from the AGP3 hybridoma (31) following a previously described method (32). Primers used in the cloning of V_L-Cκ and V_H-C_{H1} are as follows: sense V_L-Cκ, 5′-tgctggggcccagccggccgatattgtgttgacgcaggct-3′; antisense V_L-Cκ, 5′-ccgctcgagacactcattcctgttgaagct-3′; sense V_H-C_{H1}, 5′-gaagatctgaagtgcagctggtggagtct-3′; antisense V_H-C_{H1}, 5′-caggtcgacagctggaatgggcacatgcag-3′.

The V_L-Cκ and V_H-C_{H1} genes were joined by an internal ribosomal entry site and fused to the C-like extracellular, transmembrane, and cytosolic domains of the human LDLR or a truncated LDLR (ΔLDLR) lacking the NPXY signal motif to form αPEG-LDLR and αPEG-ΔLDLR, respectively. The αPEG-LDLR and αPEG-ΔLDLR sequences were then inserted into the pLNCX retroviral vector (Clontech), using the *Sfi*I and *Cla*I restriction sites, to generate pLNCX-αPEG-LDLR and pLNCX-αPEG-ΔLDLR, respectively. Recombinant retroviral particles were produced by cotransfection of pVSVG with pLNCX-αPEG-LDLR or pLNCX-αPEG-ΔLDLR into GP2-293 cells (Clontech, BD Biosciences) with Lipofectamine 2000 (Invitrogen). After 48 hours, the culture medium was filtered, mixed with 8 μg/mL polybrene (Sigma-Aldrich), and added to HCC36 cells. Following retroviral transduction for 48 hours, the cells were selected in G418 and sorted on a flow cytometer to generate HCC36/αPEG-LDLR and HCC36/αPEG-ΔLDLR cells that expressed approximately equal levels of αPEG-LDLR or αPEG-ΔLDLR receptors.

Western blotting analysis

HCC36, HCC36/αPEG-LDLR, and HCC36/αPEG-ΔLDLR cells (5×10^4) were washed in PBS and heated in reducing sample buffer at 100°C for 10 minutes. The samples were electrophoresed in an 8% SDS polyacrylamide gel under reducing conditions and then transferred onto a nitrocellulose paper (Millipore). After blocking in 5% skim milk, the membrane was incubated sequentially with 1 μg/mL horseradish peroxidase–conjugated goat anti-mouse IgM μ-chain antibody (Jackson ImmunoResearch Laboratories). The blots were washed three times with PBS-T (PBS containing 0.05% Tween 20) and twice with PBS before specific bands were visualized by enhanced chemiluminescence detection according to the manufacturer's instructions (Pierce).

Flow cytometric analysis

Surface expression of the receptors was measured by staining cells with 1 μg/mL mouse anti-HA antibody, followed by 1 μg/mL FITC-conjugated goat anti-mouse IgG (Fc) (Jackson ImmunoResearch Laboratories) in PBS containing 0.05% bovine serum albumin on ice. Functional PEG binding activity of the receptors was determined by incubating the cells with 4 μmol/L PEG-quantum dot 525 (Invitrogen) in PBS containing 0.05% bovine serum albumin on ice. After removing unbound PEG-quantum dots (PEG-QD) by extensive washing in cold PBS, the surface immunofluorescence of viable cells was measured on a FACSCalibur flow cytometer (BD Biosciences) and analyzed with FlowJo V3.2 (Tree Star, Inc.)

In vitro cytotoxicity

HCC36, HCC36/αPEG-LDLR, and HCC36/αPEG-ΔLDLR cells (10^5 per well) were seeded overnight in 96-well microtiter plates. Graded concentrations of Lipo-Dox (Schering-Plough) or doxorubicin were added to the cells in triplicate at 37°C for 6 or 24 hours. The cells were subsequently washed once and incubated for an additional 48 hours in fresh culture medium. Cell viability was determined with the ATPlite assay kit following the manufacturer's instructions (Perkin-Elmer Life and Analytical Sciences). Results are expressed as percent inhibition of luminescence as compared with untreated cells by the following formula: % inhibition = 100 × (sample luminescence − background luminescence/control luminescence − background luminescence).

Imaging of receptor-mediated endocytosis by confocal microscopy

HCC36/αPEG-LDLR or HCC36/αPEG-ΔLDLR cells were incubated with 10 nmol/L PEG-QDs or 2 mg/mL Lipo-Dox in DMEM containing 10% bovine calf serum at 37°C for 3 minutes. After extensive washing, Lipo-Dox–stained cells were incubated with FITC-conjugated AGP3 antibody (2 μg/mL) in DMEM containing 10% bovine calf serum at 37°C for 3 minutes.

After extensive washing, the endocytic activity of the receptors was recorded in real time with a confocal microscope (Axiovert 200, Carl Zeiss, Inc.). To image receptor-mediated endocytosis *in vivo*, BALB/c nude mice bearing HCC36, HCC36/αPEG-LDLR, and HCC36/αPEG-ΔLDLR tumors (~100 mm^3) in their dorsum and right and left hind leg regions, respectively, were intratumorally injected with 16 pmol of PEG-QDs (n = 3) or were i.v. injected with 10 mg/kg body weight of Lipo-Dox (n = 3). Mice were killed and tumors were harvested at 4 hours after injection. After extensive washing in PBS, the endocytic activity of the receptors was observed by two-photon confocal microscopy (LSM 510 META NLO DuoScan, Carl Zeiss).

Synthesis of PEG-NIR797

CH_3-PEG_{20000}-NH_2 (Sigma) was reacted with NIR797-isothiocyanate (Sigma) at a molar ratio of 1:2 in DMF containing 0.1% triethylamine at room temperature for 1 hour. The presence of the NIR797 group was verified by UV detection, whereas primary amine groups were detected by reaction with ninhydrin/2% solution (Sigma). The reaction mixture was separated on silica gel with dichloromethane-methanol (8:2, v/v) to obtain PEG-NIR797.

In vivo optical imaging

BALB/c nude mice (n = 5) bearing HCC36, HCC36/αPEG-LDLR, and HCC36/αPEG-ΔLDLR tumors (~100 mm^3) in their dorsum and right and left hind leg regions, respectively, were i.v. injected with PEG-NIR797 (5 mg/kg body weight) and anesthetized with isoflurane (Abbott Laboratories) using a vaporizer system (A.M. 272 Bickford). The distribution and accumulation of fluorescent probe were measured by an IVIS-50 optical imaging system (Caliper Life Sciences) at 24, 48, and 72 hours after injection. The regions of interest of tumor areas were drawn and analyzed with Living Image software version 2.50 (Caliper Life Sciences).

Accumulation of Lipo-^{111}In in tumors

BALB/c nude mice bearing HCC36, HCC36/αPEG-LDLR, and HCC36/αPEG-ΔLDLR tumors (100 mm^3) in their dorsum and right and left hind leg regions, respectively, were i.v. injected with 20 μCi of Lipo-^{111}In. Mice were killed and tumors were harvested at 24 hours (n = 4), 48 hours (n = 5), and 72 hours (n = 5) after injection. The radioactivity of weighed tumors was counted on a Wallac 1470 Wizard gamma counter (Perkin-Elmer, Inc.). Results (mean ± SD) are expressed as percent of injected radioactivity per gram tissue (%ID/g).

In vivo gamma imaging

BALB/c nude mice (n = 7) bearing HCC36, HCC36/αPEG-LDLR, and HCC36/αPEG-ΔLDLR tumors (~100 mm^3) in their left shoulders and left and right hind leg regions, respectively, were i.v. injected with 80 μCi of Lipo-^{111}In and anesthetized with isoflurane using a vaporizer system. Static images were acquired at 24, 48, and 72 hours. An ECAM+ dual-head coincidence camera (Siemens) equipped with a 4-mm pinhole collimator and ICON P computer system (Siemens) was used for gamma imaging. The anesthetized mice were placed prone on the camera's pinhole collimator, and the images were acquired as a 256 × 256 matrix for 20 minutes. Regions of interest of the tumor areas were drawn and analyzed.

In vivo treatment of HCC36 tumors by Lipo-Dox

BALB/c nude mice bearing HCC36 (n = 6), HCC36/αPEG-LDLR (n = 6), or HCC36/αPEG-ΔLDLR (n = 6) tumors (~50 mm^3) in their right flanks were i.v. injected with 2.5 or 5 mg/kg body weight of Lipo-Dox or PBS once a week for 3 weeks. Treatment efficacy was monitored by measuring tumor volumes (length × width × height × 0.5) on a weekly basis.

Data analysis

The cytotoxicity of Lipo-Dox was compared by one-way ANOVA using InStat software (GraphPad Software version 3.0, GraphPad Software) with significance determined by the Student t test. *In vitro* uptake of PEG-QDs by cells was numerated from confocal microscopic images and analyzed by the Student t test. Tumor uptake of PEGylated molecules, biodistribution of Lipo-^{111}In, and therapeutic efficacies among groups were compared by the Wilcoxon rank-sum test performed after the Kruskal-Wallis test. Bonferroni correction was used to adjust significance level for multiple (3) comparisons. P value ≤ Bonferroni corrected significance level (0.05/3 = 0.0167) was considered significant.

Results

Surface display of functional αPEG receptors

The retroviral vectors pLNCX-αPEG-LDLR and pLNCX-αPEG-ΔLDLR (Fig. 1A) encode chimeric proteins in which an anti-PEG Fab fragment was fused to the C-like extracellular, transmembrane, and cytosolic domains of LDLR or a truncated LDLR (ΔLDLR) lacking the NPXY signal motif for endocytosis (27). HCC36 hepatocellular carcinoma cells were infected with recombinant retroviral particles and selected in G418 to obtain HCC36/αPEG-LDLR and HCC36/αPEG-ΔLDLR cells. Western blot analysis showed that the cells expressed αPEG-LDLR and αPEG-ΔLDLR receptors with the expected sizes of 58 and 54 kDa, respectively (Fig. 1B). The surface expression of the receptors was analyzed by immunofluorescence staining using a specific antibody to the HA epitope present at the NH_2 terminus of the receptors. Figure 1C shows that similar levels of αPEG-LDLR and αPEG-ΔLDLR receptors were expressed on HCC36 cells. To confirm the PEG binding activity of the receptors, we stained the cells with PEG-QDs. Both receptors displayed comparable PEG-binding

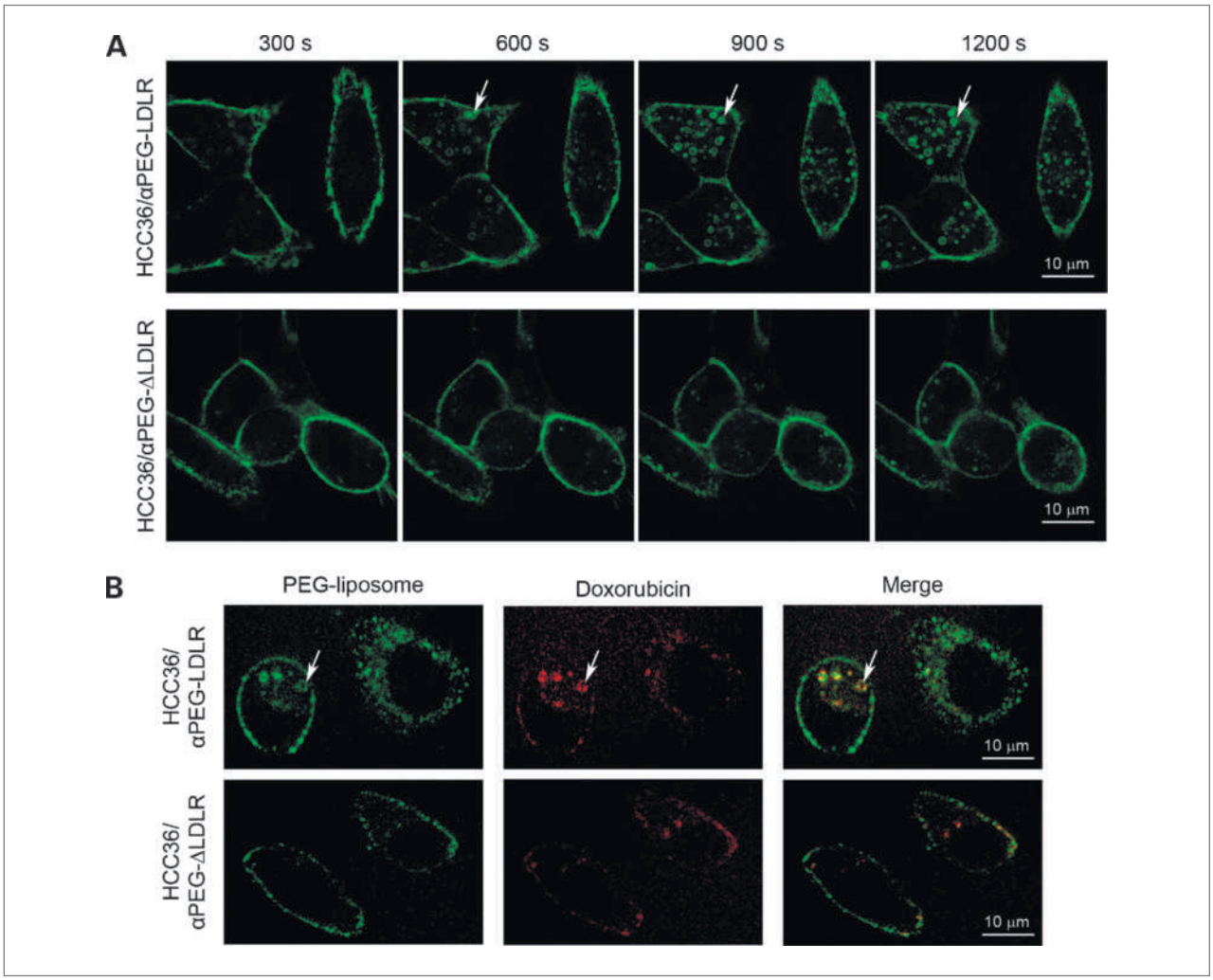

Figure 2. Real-time imaging of endocytic activity of αPEG receptors *in vitro*. A, HCC36/αPEG-LDLR (top row) and HCC36/αPEG-ΔLDLR (bottom row) cells were incubated with PEG-QDs (green fluorescence) and observed in real time with a digital confocal microscope. B, Lipo-Dox (red fluorescence) was added to HCC36/αPEG-LDLR (top row) and HCC36/αPEG-ΔLDLR (bottom row) cells, followed by a FITC-conjugated anti-PEG antibody (green fluorescence). Cells were observed with a digital confocal microscope. Merged images are shown. Arrows, endocytic vesicles. Bar, 10 μm.

activity (Fig. 1D). These results indicate that the receptors were expressed at similar levels and retained equivalent PEG-binding activities on HCC36 cells.

In vitro and *in vivo* endocytic activities of αPEG receptors

To compare the endocytic activities of the receptors, live HCC36/αPEG-LDLR and HCC36/αPEG-ΔLDLR cells were stained with PEG-QDs and then examined under a confocal microscope in real time. HCC36/αPEG-LDLR cells displayed more green fluorescence within endocytic vesicles than did HCC36/αPEG-ΔLDLR cells after PEG-QDs staining (Fig. 2A; movie available as Supplementary Material 1). On average, green fluorescent endocytic vesicles per cell were 27.3-fold (10.3 versus 0.38, $P = 0.0004$), 9.3-fold (15.1 versus 1.63, $P = 0.0003$), and 9.1-fold (17.1 versus 1.88, $P = 0.0005$) more in HCC36/αPEG-LDLR cells than in HCC36/αPEG-ΔLDLR cells at 600, 900, and 1,200 seconds after incubation of PEG-QDs, respectively. These results show that a matched pair of cells expressing endocytic and nonendocytic anti-PEG receptors was successfully established. These cells were next incubated with Lipo-Dox and then stained with a FITC-conjugated anti-PEG antibody to detect the cellular location of Lipo-Dox. Figure 2B shows that doxorubicin (red fluorescence) and PEG-liposomes (green fluorescence) colocalized within the cytoplasm of HCC36/αPEG-LDLR cells to a greater extent than in HCC36/αPEG-ΔLDLR cells, indicating that Lipo-Dox was indeed endocytosed via αPEG-LDLR receptors (movie available as Supplementary Material 2). Although we noted some doxorubicin (red fluorescence) within HCC36/αPEG-ΔLDLR cells (Fig. 2B, bottom), this doxorubicin did not colocalize with the

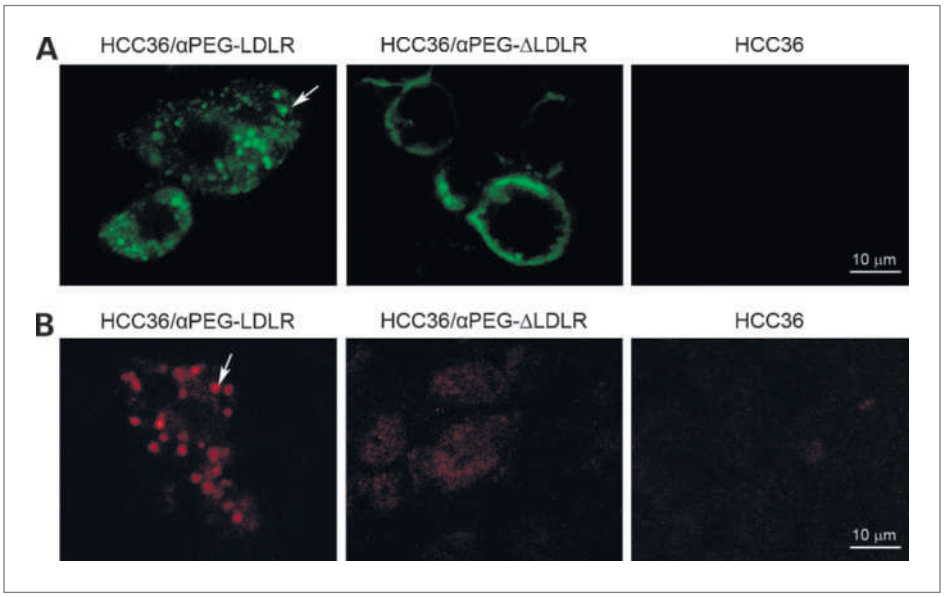

Figure 3. Receptor-mediated endocytosis of PEGylated probes and drugs *in vivo*. BALB/c nude mice bearing HCC36, HCC36/αPEG-LDLR, or HCC36/αPEG-ΔLDLR tumors were intratumorally injected with PEG-QDs ($n = 3$; A) or i.v. injected with Lipo-Dox ($n = 3$; B). Surgical tumors were observed on a two-photon confocal microscope. Arrows, endocytic vesicles. Bar, 10 μm.

PEG-liposomes (green fluorescence), suggesting that some doxorubicin may have entered the cells by diffusion. In addition, the difference in endocytic activity between αPEG-LDLR and αPEG-ΔLDLR receptors was also obvious *in vivo* as determined by two-photon confocal microscopy. Figure 3A shows that PEG-QDs accumulated intracellularly in the endocytic vesicles of HCC36/αPEG-LDLR tumors but not in HCC36/αPEG-ΔLDLR and HCC36 tumors. Similar results were also observed for the endocytosis of Lipo-Dox *in vivo* (Fig. 3B). Thus, the endocytic activity of the αPEG-LDLR receptor clearly exceeds that of the αPEG-ΔLDLR receptor *in vivo*. Collectively, these data show that endocytosis of imaging probes and therapeutic agents enhances their intracellular accumulation *in vitro* and *in vivo*.

Endocytosis enhances Lipo-Dox cytotoxicity

Lipo-Dox is now used as a preferred anticancer drug because free-form doxorubicin can produce severe cardiac toxicity (33–35). To determine whether targeting Lipo-Dox to endocytic or nonendocytic receptors would lead to differential cytotoxicity, HCC36, HCC36/αPEG-LDLR, and HCC36/αPEG-ΔLDLR cells were incubated with Lipo-Dox or free doxorubicin for 6 or 24 hours. The viability of the cells after drug treatment was determined by quantification of cellular ATP synthesis. IC_{50} values of free doxorubicin to HCC36/αPEG-LDLR, HCC36/αPEG-ΔLDLR, and HCC36 cells were 4.8, 4.2, and 3.4 μg/mL for 6-hour treatment and 0.6, 0.65, and 0.8 μg/mL for 24-hour treatment, indicating that all three cell lines displayed similar sensitivities to free doxorubicin (Fig. 4A and B). By contrast, HCC36/αPEG-LDLR cells were more sensitive to Lipo-Dox (IC_{50} = 15.5 μg/mL) than were HCC36/αPEG-ΔLDLR (IC_{50} > 54 μg/mL, $P = 0.0002$) or HCC36 cells (IC_{50} > 54 μg/mL, $P < 0.0001$) at 6-hour treatment. Treatment of HCC36/αPEG-LDLR cells with Lipo-Dox for 24 hours also caused more pronounced cytotoxicity (IC_{50} = 3.7 μg/mL) as compared with HCC36/αPEG-ΔLDLR cells (IC_{50} = 46.5 μg/mL, $P = 0.0003$) and HCC36 cells (IC_{50} > 54 μg/mL, $P < 0.0001$). In addition, similar results were also observed in a human MCF-7 breast tumor model (Supplementary Fig. S1). These data clearly show that targeting Lipo-Dox to endocytic αPEG-LDLR receptors enhances anticancer activity *in vitro*. On the other hand, addition of PEG-liposomes that do not contain doxorubicin did not induce noticeable cell death or proliferation (Supplementary Fig. S2), excluding the possibility that the presence of the NPXY motif may transduce survival-related signals.

Targeting endocytic receptors enhances cancer imaging *in vivo*

To test whether endocytosis affects imaging *in vivo*, BALB/c nude mice bearing established HCC36/αPEG-LDLR, HCC36/αPEG-ΔLDLR, and HCC36 tumors were injected with a PEGylated near-IR probe (PEG-NIR797) or Lipo-^{111}In. Whole-body images of the tumor-bearing mice were acquired by optical or gamma camera imaging, respectively, at 24, 48, and 72 hours. Figure 5A shows that, after 24 hours, HCC36/αPEG-LDLR tumors displayed more conspicuous fluorescence than did HCC36/αPEG-ΔLDLR and HCC36 tumors. Fluorescent intensities in the region of interest for HCC36/αPEG-LDLR tumors were 1.01- to 1.24-fold greater at 24 hours, 1.08- to 2.02-fold greater at 48 hours, and 1.2- to 3.54-fold greater at 72 hours than HCC36/αPEG-ΔLDLR tumors ($P < 0.009$, comparing HCC36/αPEG-LDLR with HCC36/αPEG-ΔLDLR at 48 and 72 hours), respectively (Fig. 5B). Similar results were observed for Lipo-^{111}In (Fig. 5C). Radioactivity in HCC36/αPEG-LDLR tumors

was 1.02- to 1.42-fold greater at 24 hours, 1.32- to 2.15-fold greater at 48 hours, and 1.4- to 3.9-fold greater at 72 hours than HCC36/αPEG-ΔLDLR tumors ($P < 0.0163$, comparing HCC36/αPEG-LDLR with HCC36/αPEG-ΔLDLR at 48 and 72 hours), respectively (Fig. 5D). These results show that targeting PEGylated probes or liposome to endocytic receptors can significantly enhance accumulation in tumors and improve detection sensitivity.

Targeting endocytic receptors enhances the anticancer efficacy of Lipo-Dox

To directly test the importance of receptor-mediated endocytosis of Lipo-Dox in cancer treatment, BALB/c nude mice bearing HCC36, HCC36/αPEG-LDLR, or HCC36/αPEG-ΔLDLR tumors were treated with Lipo-Dox or PBS. Tumor volumes were monitored as an indicator of Lipo-Dox efficacy. Overall, Lipo-Dox better suppressed the growth of HCC36/αPEG-LDLR tumors (Fig. 6A and B) and did not cause critical side effects (weight losses) in mice during the course of treatment (data not shown). Treating tumor-bearing mice with 2.5 mg/kg body weight of Lipo-Dox resulted in borderline differences between HCC36/αPEG-LDLR and HCC36/αPEG-ΔLDLR tumors (471.5 ± 111.7 versus 1,222.5 ± 319.2 mm^3 on day 63, $P = 0.043$; Bonferroni-corrected $P = 0.0167$). When mice were treated with 5 mg/kg Lipo-Dox, HCC36/αPEG-LDLR tumors were significantly suppressed at day 63 as compared with HCC36/αPEG-ΔLDLR tumors (63.2 ± 23.2 versus 830.4 ± 241.4 mm^3, $P = 0.0062$; Fig. 6B). Thus, our data show that targeting endocytic receptors can indeed enhance the therapeutic efficacy of Lipo-Dox *in vivo*.

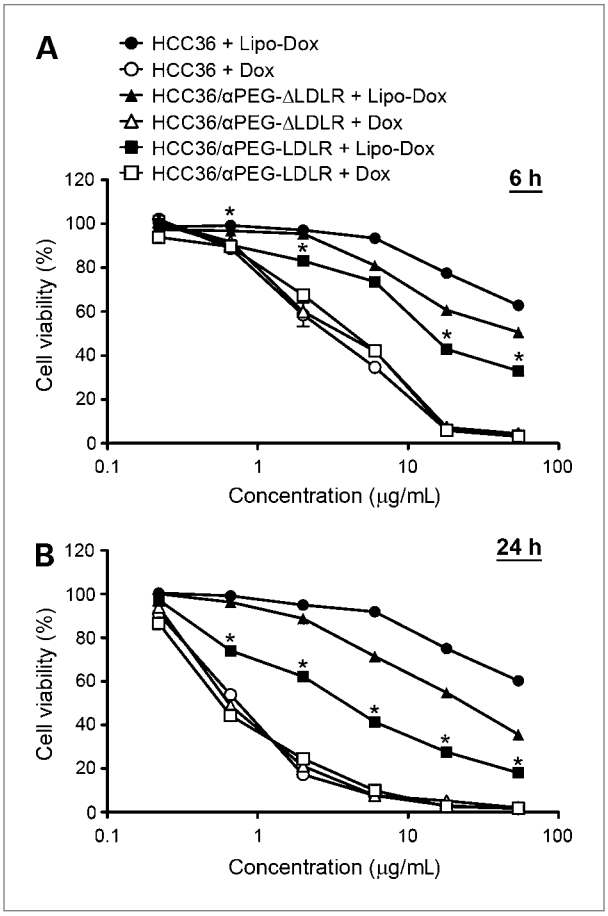

Figure 4. Endocytosis enhances Lipo-Dox cytotoxicity. HCC36/α PEG- LDLR, HCC36/αPEG-ΔLDLR, and HCC36 cells were treated with graded concentrations of Lipo-Dox or free doxorubicin in triplicate for 6 h (A) and 24 h (B). Drug-containing medium was replaced with fresh medium for an additional 48 h. Cellular ATP synthesis by the drug-treated cells was compared with that by the untreated cells, which was set as 100%. Representative data from three independent experiments are shown. Bars, SEM of triplicate determinations. *, $P \leq 0.0167$, comparing HCC36/αPEG-LDLR with HCC36/αPEG-ΔLDLR.

Discussion

By creating a matched pair of endocytic and nonendocytic receptors with specificity for any PEGylated compound, we directly and unambiguously assessed the role of endocytosis in determining the efficacy of PEGylated molecules and nanoparticles for cancer imaging and therapy. Endocytic αPEG receptors significantly increased the accumulation of PEGylated imaging probes and Lipo-Dox within tumor cells as compared with nonendocytic αPEG receptors. We observed increased accumulation of PEG-NIR797 and Lipo-^{111}In in tumors expressing endocytic αPEG receptors, which translated to stronger imaging intensity. Targeting endocytic receptors on cancer cells also significantly improved the therapeutic efficacy of Lipo-Dox both *in vitro* and *in vivo*. Thus, our study provides strong evidence that endocytosis of PEGylated imaging probes and liposomes enhances their biological activities.

The contribution of endocytosis to the efficacy of liposomal drugs has been controversial. For example, Park et al. (10) proposed that the improved anticancer efficacy of immunoliposomes was due to increased cellular internalization rather than to enhanced accumulation of liposomes at tumor sites. Sapra and Allen (20) showed that targeting immunoliposomes to internalizing CD19 molecules attained a higher therapeutic index than targeting to noninternalizing CD20 molecules on B-lymphoma cells. However, because B cells do not express similar amounts of CD19 and CD20, the relative contributions of dosage versus internalization are difficult to discern. Furthermore, on ligation with immunoliposomes, CD19 and CD20 can transduce distinct signals through different downstream effectors, which may further confound interpretation of treatment efficacies (36–39). It is therefore difficult to precisely assign the relative contribution of endocytosis in immunoliposome efficacy when using different tumor markers. To directly address this issue, we expressed on HCC36 cells endocytic or nonendocytic αPEG receptors with identical specificity. By expressing similar levels of the

receptors on cells, possible dose-related effects were avoided. Consistent with other receptors (28, 40, 41), the NPXY signal motif in the LDLR did not transduce survival-related signals after the receptors were cross-linked with PEGylated compounds. This model therefore represents an unbiased system to analyze the importance of endocytosis of Lipo-Dox in tumor therapy. By using this model, we show here that endocytosis of Lipo-Dox augments treatment efficacy.

Enhanced treatment efficacy toward HCC36 cancer cells expressing endocytic αPEG receptors is consistent with our *in vitro* and *in vivo* imaging studies. As shown in confocal microscopic studies, significantly more endosomes containing Lipo-Dox and PEG-QDs were observed in HCC36/αPEG-LDLR cells. Because HCC36/αPEG-LDLR and HCC36/αPEG-ΔLDLR initially bound similar amounts of Lipo-Dox, and these two cells were equally sensitive to free-form doxorubicin, increased cytotoxicity observed toward HCC36/αPEG-LDLR cells can be attributed to increased accumulation of intracellular Lipo-Dox. Likewise, tracking the accumulation of PEGylated probes in tumors expressing endocytic or nonendocytic αPEG receptors by optical and gamma camera imaging showed stronger signals within HCC36/αPEG-LDLR tumors, which correlated with higher therapeutic index against these tumors after Lipo-Dox treatment.

Our data also indicate that endocytosis of imaging probes enhances detection sensitivity. Signal intensity in HCC36/αPEG-LDLR tumors was significantly greater than that in HCC36/αPEG-ΔLDLR tumor by both optical imaging and gamma camera. In addition, it is interesting that the difference in imaging intensity between the endocytic and the nonendocytic cells was only significant at 48 and 72 hours, but not at 24 hours. This suggests

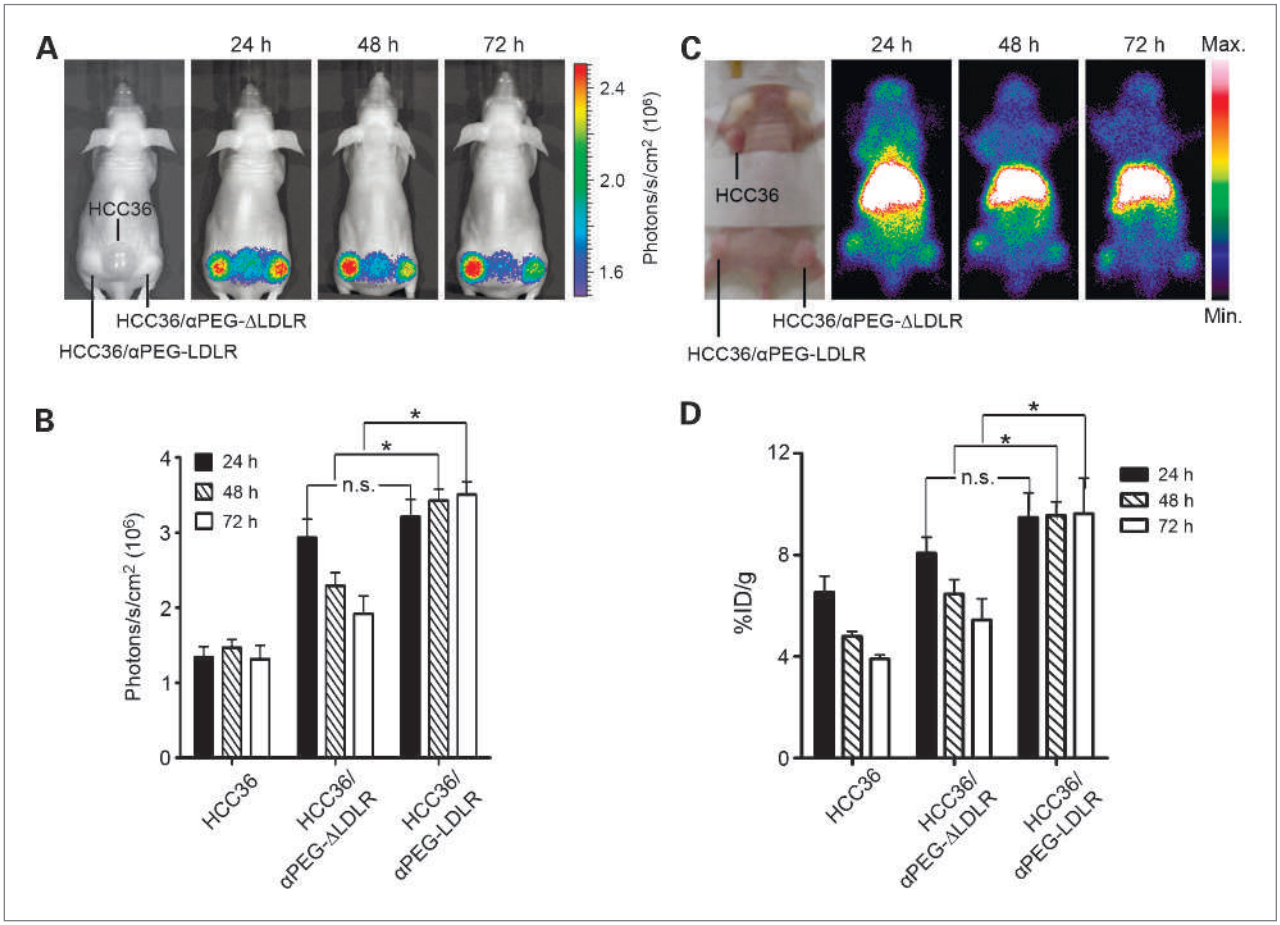

Figure 5. Targeting endocytic receptors enhances cancer imaging *in vivo*. A, BALB/c nude mice (n = 5) bearing HCC36 (middle), HCC36/αPEG-LDLR (left hind limb), and HCC36/αPEG-ΔLDLR (right hind limb) tumors were i.v. injected with PEG-NIR797 (5 mg/kg body weight), and images acquired on an IVIS-50 optical imaging system at 24, 48, and 72 h after injection. B, optical intensity in tumors after i.v. injection of PEG-NIR797 was analyzed with Living Image software version 2.50. Points, mean; bars, SEM. C, BALB/c nude mice (n = 7) bearing HCC36 (left shoulder), HCC36/αPEG-LDLR (left hind limb), and HCC36/αPEG-ΔLDLR (right hind limb) tumors were i.v. injected with 80 μCi of Lipo-^{111}In, and images acquired at 24, 48, and 72 h after injection by a gamma camera. D, accumulation of Lipo-^{111}In in tumors by measuring radioactivity of weighted tumors at 24 h (n = 4), 48 h (n = 5), and 72 h (n = 5). Data are expressed as percent injected dose per gram of tissue (%ID/g tissue). *, $P \leq 0.0167$, between αPEG-LDLR and αPEG-ΔLDLR tumors. n.s., not significant. Columns, mean; bars, SEM.

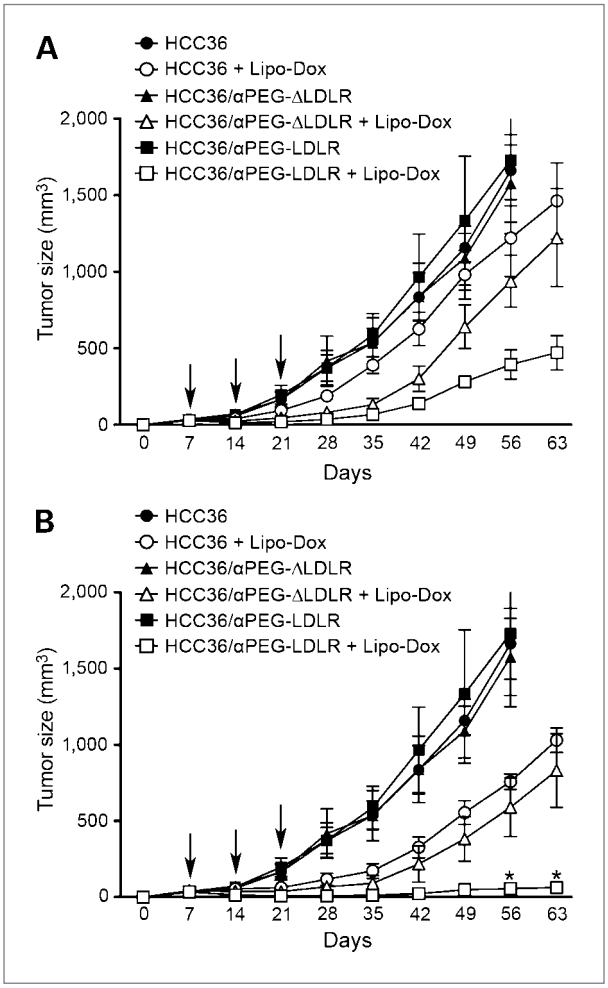

Figure 6. Targeting endocytic receptors enhances the anticancer efficacy of Lipo-Dox. BALB/c nude mice bearing HCC36 (n = 6), HCC36/αPEG-LDLR (n = 6), or HCC36/αPEG-ΔLDLR (n = 6) tumors were i.v. injected with Lipo-Dox at 2.5 mg/kg (A) or 5 mg/kg (B) once per week for 3 wk. Control tumor-bearing mice received PBS alone. *, $P \leq 0.0167$, between αPEG-LDLR and αPEG-ΔLDLR tumors. Arrows, treatment schedule. Points, mean; bars, SEM.

that both HCC36/αPEG-LDLR and HCC36/αPEG-ΔLDLR tumors can trap PEGylated imaging probes. However, HCC36/αPEG-LDLR tumors are able to internalize the imaging probes, which enhanced the imaging signal over time. Based on these reasons, the stronger signal observed in HCC36/αPEG-LDLR tumors suggests that targeting imaging probes to endocytic tumor markers may aid in detection and diagnosis of smaller tumors *in vivo*. Moreover, both PEG-NIR797 and Lipo-^{111}In were endocytosed by the αPEG-LDLR receptor, suggesting that both small-molecule probes and nanoparticles can be conjugated to tumor-targeting ligands for enhanced cancer imaging.

Our observation that endocytosis of imaging probes or liposomal drugs enhances their efficacy may directly affect the future design of more effective imaging probes and anticancer drugs. Based on our data, nanoparticles and macromolecular agents should be designed to target endocytic tumor markers. By combining the benefits of selective targeting and increased intracellular accumulation, this design strategy should produce superior effects over nonendocytic tumor markers.

We provide direct and unbiased *in vitro* and *in vivo* evidence that targeted endocytosis of PEG-liposomal drugs and PEG-imaging probes can improve antitumor efficacy and enhance tumor imaging. These results also suggest that future design of immunoliposomes and targeted imaging agents should focus on endocytic epitopes to achieve more effective tumor therapy. Finally, the universal anti-PEG receptors described here may form the basis for genetic marking of tissues to facilitate detection or treatment by any PEGylated compound or nanoparticle.

Disclosure of Potential Conflicts of Interest

No potential conflicts of interest were disclosed.

Acknowledgments

The authors acknowledge technical support from the Molecular and Genetic Imaging Core supported by the National Research Program for Genomic Medicine, National Science Council, Taiwan (NSC98-3112-B-037-001), the Scientific Instrument Center of Academia Sinica, the Kaohsiung Medical University Hospital Cancer Center (DOH99-TD-C-111-002), and the National Sun Yat-Sen University-Kaohsiung Medical University Joint Research Center.

Grant Support

The National Research Program for Genomic Medicine (NSC98-3112-B-037-001; T.L. Cheng), the National Health Research Institutes (NHRI-EX98-9624SI; T.L. Cheng), and Academia Sinica (AS-98-TP-B09; S.R. Roffler).

The costs of publication of this article were defrayed in part by the payment of page charges. This article must therefore be hereby marked *advertisement* in accordance with 18 U.S.C. Section 1734 solely to indicate this fact.

Received 10/06/2009; revised 03/11/2010; accepted 04/12/2010; published OnlineFirst 05/25/2010.

References

1. Papahadjopoulos D, Allen TM, Gabizon A, et al. Proc Natl Acad Sci U S A 1991;88:11460–4.
2. Allen TM, Cullis PR. Drug delivery systems: entering the mainstream. Science 2004;303:1818–22.
3. Torchilin VP. Recent advances with liposomes as pharmaceutical carriers. Nat Rev Drug Discov 2005;4:145–60.
4. Allen TM, Hansen C, Martin F, Redemann C, Yau-Young A. Liposomes containing synthetic lipid derivatives of poly(ethylene glycol) show prolonged circulation half-lives *in vivo*. Biochim Biophys Acta 1991;1066:29–36.
5. Klibanov AL, Maruyama K, Torchilin VP, Huang L. Amphipathic polyethyleneglycols effectively prolong the circulation time of liposomes. FEBS Lett 1990;268:235–7.
6. Hsiao SM, Chen CA, Lin HH, Hsieh CY, Wei LH. Phase II trial of carboplatin and distearoylphosphatidylcholine pegylated liposomal doxorubicin (Lipo-Dox) in recurrent platinum-sensitive ovarian cancer

following front-line therapy with paclitaxel and platinum. Gynecol Oncol 2009;112:35–9.
7. Chao TC, Wang WS, Yen CC, Chiou TJ, Liu JH, Chen PM. A dose-escalating pilot study of sterically stabilized, pegylated liposomal doxorubicin (Lipo-Dox) in patients with metastatic breast cancer. Cancer Invest 2003;21:837–47.
8. Lo A, Lin CT, Wu HC. Hepatocellular carcinoma cell-specific peptide ligand for targeted drug delivery. Mol Cancer Ther 2008;7:579–89.
9. Lee TY, Lin CT, Kuo SY, Chang DK, Wu HC. Peptide-mediated targeting to tumor blood vessels of lung cancer for drug delivery. Cancer Res 2007;67:10958–65.
10. Park JW, Hong K, Kirpotin DB, et al. Anti-HER2 immunoliposomes: enhanced efficacy attributable to targeted delivery. Clin Cancer Res 2002;8:1172–81.
11. Sugano M, Egilmez NK, Yokota SJ, et al. Antibody targeting of doxorubicin-loaded liposomes suppresses the growth and metastatic spread of established human lung tumor xenografts in severe combined immunodeficient mice. Cancer Res 2000;60:6942–9.
12. Roth A, Drummond DC, Conrad F, et al. Anti-CD166 single chain antibody-mediated intracellular delivery of liposomal drugs to prostate cancer cells. Mol Cancer Ther 2007;6:2737–46.
13. An F, Drummond DC, Wilson S, et al. Targeted drug delivery to mesothelioma cells using functionally selected internalizing human single-chain antibodies. Mol Cancer Ther 2008;7:569–78.
14. Hussain S, Pluckthun A, Allen TM, Zangemeister-Wittke U. Antitumor activity of an epithelial cell adhesion molecule targeted nanovesicular drug delivery system. Mol Cancer Ther 2007;6:3019–27.
15. Madhankumar AB, Slagle-Webb B, Mintz A, Sheehan JM, Connor JR. Interleukin-13 receptor-targeted nanovesicles are a potential therapy for glioblastoma multiforme. Mol Cancer Ther 2006;5:3162–9.
16. Harashima H, Tsuchihashi M, Iida S, Doi H, Kiwada H. Pharmacokinetic/pharmacodynamic modeling of antitumor agents encapsulated into liposomes. Adv Drug Deliv Rev 1999;40:39–61.
17. Harashima H, Iida S, Urakami Y, Tsuchihashi M, Kiwada H. Optimization of antitumor effect of liposomally encapsulated doxorubicin based on simulations by pharmacokinetic/pharmacodynamic modeling. J Control Release 1999;61:93–106.
18. Vingerhoeds MH, Steerenberg PA, Hendriks JJ, et al. Immunoliposome-mediated targeting of doxorubicin to human ovarian carcinoma *in vitro* and *in vivo*. Br J Cancer 1996;74:1023–9.
19. Lim HJ, Masin D, McIntosh NL, Madden TD, Bally MB. Role of drug release and liposome-mediated drug delivery in governing the therapeutic activity of liposomal mitoxantrone used to treat human A431 and LS180 solid tumors. J Pharmacol Exp Ther 2000;292:337–45.
20. Sapra P, Allen TM. Internalizing antibodies are necessary for improved therapeutic efficacy of antibody-targeted liposomal drugs. Cancer Res 2002;62:7190–4.
21. Huang A, Kennel SJ, Huang L. Interactions of immunoliposomes with target cells. J Biol Chem 1983;258:14034–40.
22. Robinson MK, Doss M, Shaller C, et al. Quantitative immuno-positron emission tomography imaging of HER2-positive tumor xenografts with an iodine-124 labeled anti-HER2 diabody. Cancer Res 2005;65:1471–8.
23. Wen X, Wu QP, Ke S, et al. Conjugation with ^{111}In-DTPA-poly(ethylene glycol) improves imaging of anti-EGF receptor antibody C225. J Nucl Med 2001;42:1530–7.
24. Peng L, Liu R, Andrei M, Xiao W, Lam KS. *In vivo* optical imaging of human lymphoma xenograft using a library-derived peptidomimetic against $\alpha_4\beta_1$ integrin. Mol Cancer Ther 2008;7:432–7.
25. Falciani C, Fabbrini M, Pini A, et al. Synthesis and biological activity of stable branched neurotensin peptides for tumor targeting. Mol Cancer Ther 2007;6:2441–8.
26. Liu Z, Liu S, Wang F, Chen X. Noninvasive imaging of tumor integrin expression using ^{18}F-labeled RGD dimer peptide with PEG(4) linkers. Eur J Nucl Med Mol Imaging 2009;36:1296–307.
27. Chen WJ, Goldstein JL, Brown MS. NPXY, a sequence often found in cytoplasmic tails, is required for coated pit-mediated internalization of the low density lipoprotein receptor. J Biol Chem 1990;265:3116–23.
28. Bansal A, Gierasch LM. The NPXY internalization signal of the LDL receptor adopts a reverse-turn conformation. Cell 1991;67:1195–201.
29. Hsieh YJ, Chang CH, Huang SP, et al. Effect of cyclosporin A on the brain regional distribution of doxorubicin in rats. Int J Pharm 2008;350:265–71.
30. Chow TH, Lin YY, Hwang JJ, et al. Diagnostic and therapeutic evaluation of ^{111}In-vinorelbine-liposomes in a human colorectal carcinoma HT-29/luc-bearing animal model. Nucl Med Biol 2008;35:623–34.
31. Cheng TL, Wu PY, Wu MF, Chern JW, Roffler SR. Accelerated clearance of polyethylene glycol-modified proteins by anti-polyethylene glycol IgM. Bioconjug Chem 1999;10:520–8.
32. Roffler SR, Wang HE, Yu HM, et al. A membrane antibody receptor for noninvasive imaging of gene expression. Gene Ther 2006;13:412–20.
33. Forssen EA, Tokes ZA. Use of anionic liposomes for the reduction of chronic doxorubicin-induced cardiotoxicity. Proc Natl Acad Sci U S A 1981;78:1873–7.
34. Gabizon A, Meshorer A, Barenholz Y. Comparative long-term study of the toxicities of free and liposome-associated doxorubicin in mice after intravenous administration. J Natl Cancer Inst 1986;77:459–69.
35. van Hoesel QG, Steerenberg PA, Crommelin DJ, et al. Reduced cardiotoxicity and nephrotoxicity with preservation of antitumor activity of doxorubicin entrapped in stable liposomes in the LOU/M Wsl rat. Cancer Res 1984;44:3698–705.
36. Fujimoto M, Poe JC, Jansen PJ, Sato S, Tedder TF. CD19 amplifies B lymphocyte signal transduction by regulating Src-family protein tyrosine kinase activation. J Immunol 1999;162:7088–94.
37. Callard RE, Rigley KP, Smith SH, Thurstan S, Shields JG. CD19 regulation of human B cell responses. B cell proliferation and antibody secretion are inhibited or enhanced by ligation of the CD19 surface glycoprotein depending on the stimulating signal used. J Immunol 1992;148:2983–7.
38. Hofmeister JK, Cooney D, Coggeshall KM. Clustered CD20 induced apoptosis: src-family kinase, the proximal regulator of tyrosine phosphorylation, calcium influx, and caspase 3-dependent apoptosis. Blood Cells Mol Dis 2000;26:133–43.
39. van der Kolk LE, Evers LM, Omene C, et al. CD20-induced B cell death can bypass mitochondria and caspase activation. Leukemia 2002;16:1735–44.
40. Kibbey RG, Rizo J, Gierasch LM, Anderson RG. The LDL receptor clustering motif interacts with the clathrin terminal domain in a reverse turn conformation. J Cell Biol 1998;142:59–67.
41. Uhlik MT, Temple B, Bencharit S, Kimple AJ, Siderovski DP, Johnson GL. Structural and evolutionary division of phosphotyrosine binding (PTB) domains. J Mol Biol 2005;345:1–20.